

## Pumping of water with ac electric fields applied to asymmetric pairs of microelectrodes

A. B. D. Brown,<sup>1,\*</sup> C. G. Smith,<sup>1,†</sup> and A. R. Rennie<sup>2,‡</sup>

<sup>1</sup>*Semiconductor Physics, Cavendish Laboratory, Madingley Road, Cambridge, CB3 0HE, United Kingdom*

<sup>2</sup>*Department of Chemistry, Kings College London, Strand, London WC2R 2LS, United Kingdom*

(Received 31 July 2000; published 20 December 2000)

Bulk fluid flow induced by an ac electric potential with a peak voltage below the ionization potential of water is described. The potential is applied to an ionic solution with a planar array of electrodes arranged in pairs so that one edge of a large electrode is close to an opposing narrow electrode. During half the cycle, the double layer on the surface of the electrodes charges as current flows between the electrodes. The electrodes charge in a nonuniform manner producing a gradient in potential parallel to the surface of the electrodes. This gradient drives the ions in the double layer across the surface of the electrode and this in turn drags the fluid across the electrode surface. The anisotropic nature of the pairs of electrodes is used to produce a net flow of fluid. The flow produced is approximately uniform at a distance from the electrodes that is greater than the periodicity of the electrode array. The potential and frequency dependence of this flow is reported and compared to a simple model. This method of producing fluid flow differs from electrical and thermal traveling-wave techniques as only a low voltage is required and the electrode construction is much simpler.

DOI: 10.1103/PhysRevE.63.016305

PACS number(s): 47.65.+a, 83.60.Np, 82.45.+z, 85.90.+h

### I. INTRODUCTION

Interest in controlling the movement of small volumes of fluid has been growing rapidly in recent years. This is important in the field of biotechnology as single cells and their surrounding fluid need to be manipulated. Micromachines are also being developed and it is expected that they will play significant roles in diverse areas such as analytical probes, drug delivery systems, and surgical tools. To perform these tasks means are required to pump fluids either as a mechanism of propulsion for the micromachines, or to move materials across the surface of an analytical probe. Currently there are several means by which microscopic pumps can be achieved. These include the use of thermal gradients [1], electric fields [1], magnetic fields [2,3], as well as electromechanical means such as piezoelectric actuators [4].

Recently pairs of microelectrodes subjected to alternating electric fields have been reported to drive a new type of fluid flow [5–8]. The mechanism has involved creation of vortices and these have been used to move fluids and cluster particles over the surface of an electrode. This technique has not been used to produce a net flow of fluid over an entire electrode array. However, it has been suggested [9] that a net flow could be driven with an array of electrodes that are modified so that each electrode is anisotropic in shape, potential, or capacitance. In this way each electrode produces an anisotropic force on ions in a fluid that can drive the flow across the electrodes.

In this paper net fluid flow is produced using a related method. Pairs of electrodes are fabricated so that, as a pair, they are anisotropic in shape and thus provide a direction in which the fluid is pumped. The present paper describes a

simple theoretical model that describes the movement of ions in an aqueous solution near the surface of an electrode. It is assumed that these ions drag solvating water molecules thus producing fluid flow. This theory is compared with the electrical response of the electrode array and observations of the fluid flow. The flow is observed by tracking the motion of colloidal particles with an optical microscope as they move with the fluid.

### II. EXPERIMENT

An array of interdigitated electrodes was built consisting of a small electrode (4.2  $\mu\text{m}$  wide) separated from the large electrode (25.7  $\mu\text{m}$  wide) by a 4.5  $\mu\text{m}$  gap. Pairs of such electrodes were repeated at 50  $\mu\text{m}$  intervals, leaving a gap of 15.6  $\mu\text{m}$  between the small electrode in one pair and the large electrode in the next pair. The shape of the grid was defined using photolithography and contained 130 repeats. It was made by evaporating 10 nm of Nichrome and then 100 nm of gold onto a glass slide, patterned with photoresist. The purpose of the Nichrome was to provide good adhesion with the glass. Gold was chosen as the electrode material rather than titanium [5], as gold does not form an oxide layer in water which would add to the surface capacitance. The cell was then assembled as shown in Fig. 1, and the sample was viewed in dark field under reflected light. The electrodes were driven using a lock-in amplifier which allowed the measurement of the complex impedance of the cell.

The sample investigated was a very dilute dispersion ( $\sim 0.0005$  v/v) of 0.5  $\mu\text{m}$  polystyrene latex spheres in  $10^{-4}$  M solution of  $\text{NaNO}_3$ . These particles were observed to move above the electrodes. The velocity of the fluid was measured by capturing images of the particles over the grid at regular time intervals and then using these images to track the motion of the particles. The distance between the particles observed and the electrodes was controlled by adjusting the focus of the microscope. The range of distances observed depended upon the depth of field of the objective and the

\*Email address: ben@brownshouse.com

†FAX: +44 1223 337271. Email address: cgs4@cam.ac.uk

‡FAX: +44 207 8482810. Email address: rennie@colloids.ch.kcl.ac.uk

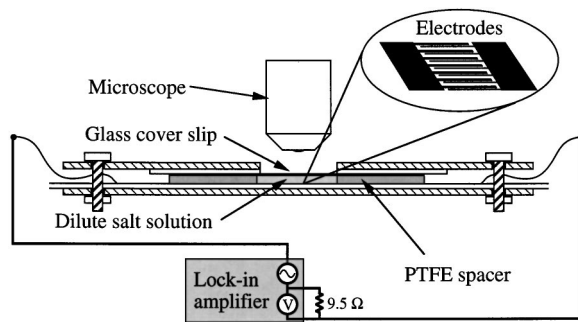


FIG. 1. A cross section of the cell used. The PTFE spacer provided a gap of  $340\ \mu\text{m}$  above the electrodes which was completely filled with solution. The electrodes were driven with a lock-in amplifier that allowed the impedance of the cell to be measured.

acceptance levels allowed by the analyzing program. Typically particles were accepted within a range of approximately  $\pm 10\ \mu\text{m}$ .

### III. MEASURED FLUID VELOCITIES

When an ac field was applied to the electrodes, the particles were observed to move perpendicular to the length of the electrodes. The direction of motion was away from the small electrode, across the narrow gap, towards the large electrode, i.e., from the near (bottom) to the far (top) side as the electrode grid is shown in Fig. 1. It is assumed that the particles move with the fluid, and so can be used to measure the motion of the fluid. In general this is not true, as the particles are charged, and so will experience an electrostatic force. However, as long as the time over which the particles are observed is longer than the period of the applied potential, this force will average to zero and have no effect. In high field gradients, particles will also experience a force arising from the difference between their dielectric properties and that of the surrounding water. Again this effect is not expected to be significant in this experiment where the voltages are in the region of 1 V and particles are tracked at large distances from the electrode surfaces where the highest field gradients are located.

Figure 2 shows the velocity of the fluid as it varies with height above the electrodes. The distance from the electrodes to the bottom surface of the cover slip was found to be  $340\ \mu\text{m}$ . The flow rate has been fitted with a quadratic function, and constrained to have no velocity at the upper surface of the fluid. The flow rate does not vary linearly with height due to the pressure distribution generated within the cell by the flow. The shape of the curve is simply dependent on the ratio between the pressure and the velocity of the fluid. This curve can be extrapolated to the surface of the electrodes to give a fluid velocity that would be observed if there was no back pressure generated, and if the top surface of the fluid was not constrained to be stationary. Assuming the fluid flow is laminar at all flow rates investigated, the shape of the curve will remain the same for all pumping velocities. This means that the ratio between the velocity in the absence of back pressure, and the observed velocity at a given distance will remain constant for all pumping rates.

At distances below  $50\ \mu\text{m}$  the tracer particles were observed to move out of focus and then back into focus as they

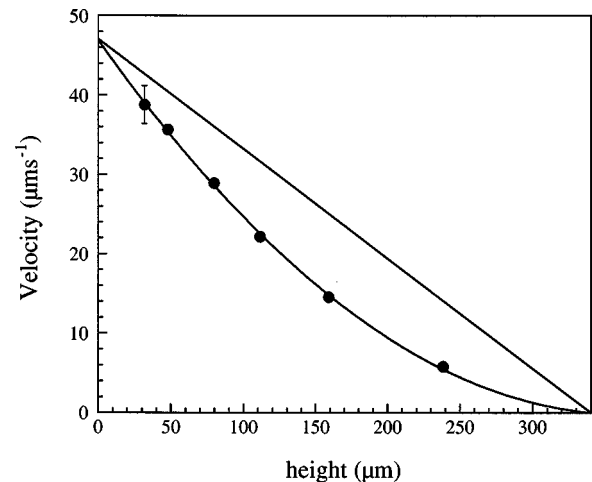


FIG. 2. Observed fluid velocity as it varies with distance above the surface of the electrodes. Error bars are shown where the error is larger than the point size. The data points have been fitted with a quadratic function. This is the form expected if a back pressure is present. The straight line is the profile that would be expected in the absence of any back pressure. The curve is extrapolated to the surface of the electrode to give the velocity that would be observed in the absence of any back pressure and in the absence of an upper static boundary condition.

moved across the electrode array. This shows that near the electrodes the flow is not simply in a horizontal plane, but has vertical components as well. This vertical velocity made it difficult to track the motion of particles, and so all further measurements were made at a height of  $80\ \mu\text{m}$  above the electrodes. In order to make measurements from different experiments comparable, the velocities measured were scaled to give the velocity in the absence of back pressure.

Figure 3 shows the fluid velocity as it varies with applied frequency at an applied voltage of  $0.8\ \text{V}_{\text{rms}}$  at 1 h intervals, before, during, and after the other measurements were made. The velocity decreases slightly with use of the electrode. When the electrodes were viewed after the experiment, the

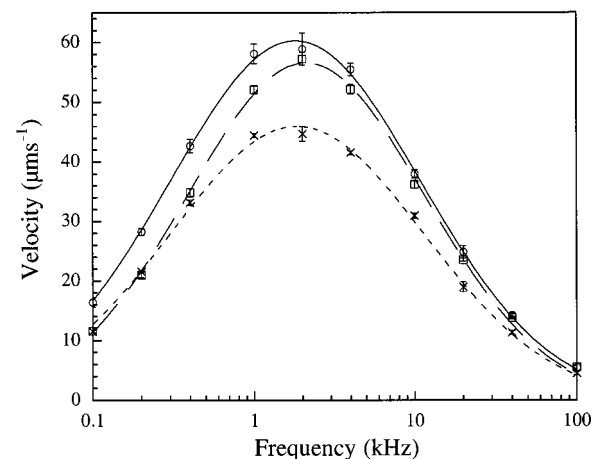


FIG. 3. The scaled fluid velocity plotted against applied frequency at a potential of  $0.8\ \text{V}_{\text{rms}}$ , before the experiment ( $\circ$ ), during the experiment ( $\square$ ), and after the experiment ( $\times$ ), at approximately 1 h intervals. The fitted Gaussian curves are to aid the eye.

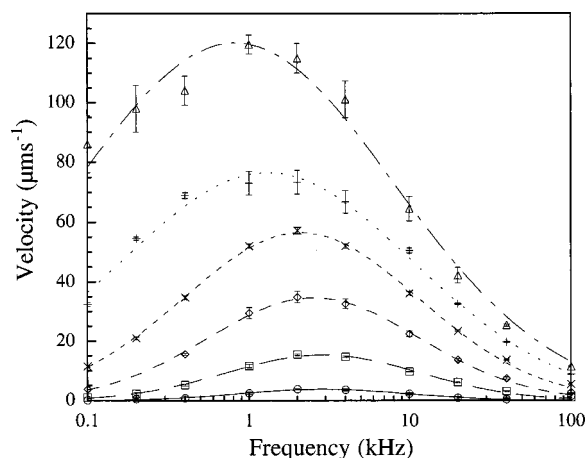


FIG. 4. The scaled fluid velocity plotted against the applied frequency at six different values of the applied potential:  $0.2 V_{\text{rms}}$  ( $\circ$ ),  $0.4 V_{\text{rms}}$  ( $\square$ ),  $0.6 V_{\text{rms}}$  ( $\diamond$ ),  $0.8 V_{\text{rms}}$  ( $\times$ ),  $1.0 V_{\text{rms}}$  ( $+$ ), and  $1.2 V_{\text{rms}}$  ( $\triangle$ ). The fitted Gaussian curves are to aid the eye.

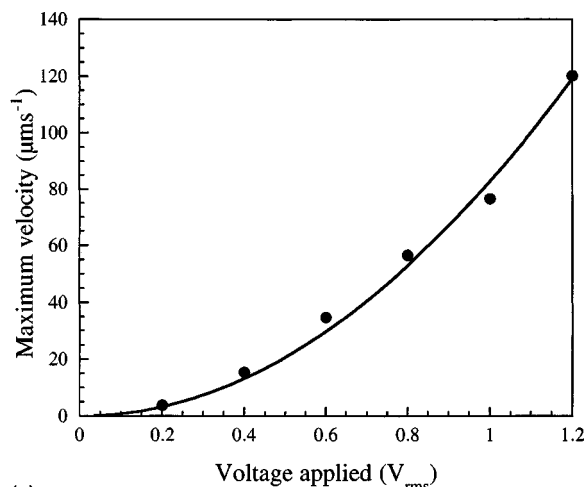
narrow electrode appeared slightly roughened and spheres were observed to have deposited on the electrodes, particularly on the small electrode.

Figure 4 shows the fluid velocity as it varies with applied frequency for different values of the applied voltage. The curves have been fitted with a Gaussian with no background, and the variation of peak height and peak position with applied voltage are shown in Figs. 5(a) and 5(b). The peak increases in size and moves to lower frequency as the amplitude of the applied signal is increased.

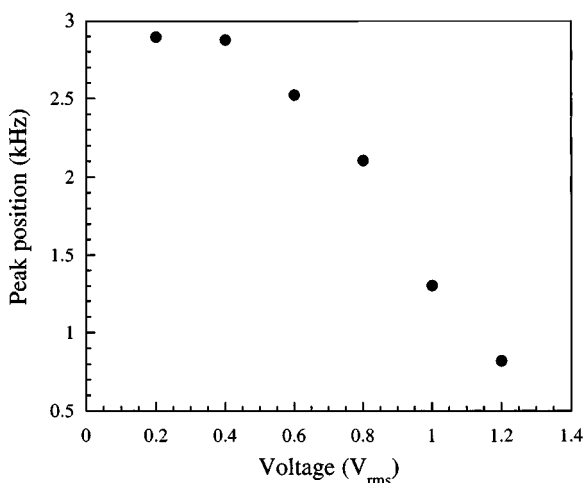
#### IV. THEORETICAL MODEL

Consider two infinitely long electrodes of different widths placed next to each other on a nonconducting substrate immersed in an aqueous solution as shown in Fig. 6(a). If an ac potential is applied to these electrodes then a current will be induced in the solution. If the frequency is low enough so that ions can equilibrate locally (i.e., below  $\sim 10$  MHz for  $10^{-4}$  mol dm $^{-3}$  monovalent salt), and if the applied potential is below the ionization potential, so that electrolysis does not occur at the electrode surfaces, then the bulk water will behave in a resistive manner. At the electrode surfaces a double layer with a separation of charge will form. This double layer will behave in a capacitive manner. When a potential is applied, and if the distortion of the field lines at the edges of the electrodes is ignored, the field lines are approximately semicircular. Away from the surface of the electrodes the current will flow parallel to the field lines from one electrode to the other. As it does so, the amount of charge separated in the double layers increases. If the fluid is divided up into tubes parallel to the field lines and terminating at the electrodes, then these tubes can each be modeled by a resistor with a capacitor at each end as shown in Fig. 6(b).

Let the large electrode have width  $L$  and the small electrode width  $S$  and let the gap between them be  $G$  as illustrated in Fig. 6(a). In order to simplify the algebra it is useful to have a variable  $x$  that describes the position of both ends of a conduction path across the surface of the electrodes. Let



(a)



(b)

FIG. 5. (a) The maximum velocity plotted against applied voltage ( $\psi$ ) fitted with  $v = B\psi^2$  where  $B$  is a constant as predicted in Eq. (1). (b) The frequency at which the velocity is a maximum plotted against applied voltage.

the ratio of the electrode widths (i.e.,  $L/S$ ) be  $k$ . Let an origin be chosen between the electrodes such that a conduction path that starts at a distance of  $x\sqrt{k}$  from this origin over the large electrode will end at a point  $x/\sqrt{k}$  from this origin over the small electrode. Let  $x_{\text{min}}$  and  $x_{\text{max}}$  be chosen such that the large electrode lies between points  $x_{\text{min}}\sqrt{k}$  and  $x_{\text{max}}\sqrt{k}$  from the origin and the small electrode lies between points  $x_{\text{min}}/\sqrt{k}$  and  $x_{\text{max}}/\sqrt{k}$  from that same origin, as shown in Fig. 6(a). This means that  $x_{\text{min}}$  is equal to  $G/(\sqrt{k} + 1/\sqrt{k})$ , and  $x_{\text{max}}$  is equal to  $(G + L + S)/(\sqrt{k} + 1/\sqrt{k})$ . Using this notation the electrode array used in the experiment described above has values of  $k = 6.12$ ,  $x_{\text{min}} = 1.6 \mu\text{m}$ , and  $x_{\text{max}} = 12.0 \mu\text{m}$  for each pair of electrodes.

Assuming the field lines are approximately semicircular, a tube of thickness  $\delta x\sqrt{k}$  over the large electrode, at a point distance  $x\sqrt{k}$  from the origin, will reach the small electrode at a point  $x/\sqrt{k}$  from the origin where it will have a thickness  $\delta x/\sqrt{k}$ . The resistance  $R(x)$  of this tube per unit length of electrode is given by

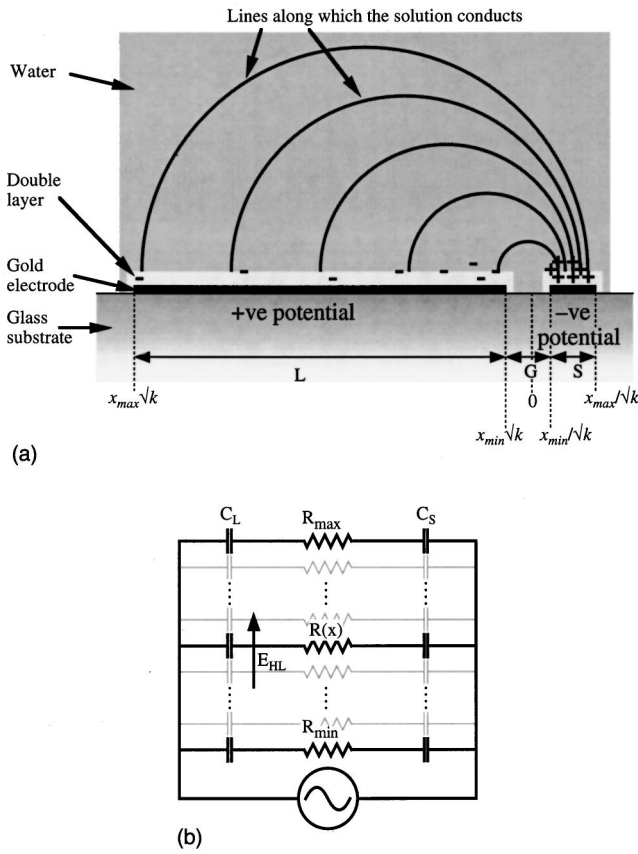


FIG. 6. (a) A pair of differently sized gold electrodes on a glass substrate in water at the instant that the large electrode is at a positive potential and the small electrode is at a negative potential. The continuous lines indicate the direction of the field lines along which the solution conducts. (b) The equivalent electrical circuit. The double layer acts as a capacitor while the bulk of the water acts as a resistor. The value of the resistance varies from  $R_{\min}$  between the near edges of the electrodes to  $R_{\max}$  between the far edges of the electrodes.

$$R(x) = \frac{\pi x (\sqrt{k} + 1/\sqrt{k})}{2\sigma \delta x}$$

where  $\sigma$  is the conductivity of the solution.

The distribution of charge at a surface will follow a solution of the Poisson-Boltzmann equation. Some ions may be tightly bound in a Stern layer while the rest are distributed in a diffuse layer characterized by a screening distance  $\lambda_D$  [10].

The distance by which charge is separated in the Stern layer is very small. However, only a limited amount of charge can dwell in this layer. At present there is no model that satisfactorily predicts the nature of the Stern layer as it is dependent upon the ion species, electrode material, and applied potential.

In the limit of a small applied potential ( $<25$  mV) the screening distance or thickness of the diffuse layer is given by the Debye-Hückel approximation [10], giving 30 nm for a  $10^{-4}$  mol dm $^{-3}$  solution of monovalent ions, and is indepen-

dent of the applied voltage. However, when larger potentials are placed across the interface, the diffuse layer compresses.

It is not clear how the capacitance of the Stern layer and the diffuse layer might combine. In the following calculation it is assumed that the total capacitance can be described by an effective value of  $\lambda_D$  for a given applied amplitude. It is also assumed that all the ions in this separation of charge are mobile. The capacitance of the double layer at each end of the tube per unit length of the electrode is therefore given by

$$C_{DL} = \varepsilon \delta x \sqrt{k} / \lambda_D$$

at the large electrode and

$$C_{DS} = \varepsilon \delta x / \sqrt{k} \lambda_D$$

at the small electrode, where  $\varepsilon$  is the permittivity of water.

If a potential  $\Psi = \Psi_0 \exp(i\omega t)$  is applied to the electrodes then the potential across the double layer on the large electrode  $\Psi_{DL}$  will vary as

$$\Psi_{DL}(x) = \Psi - IR - \frac{I}{i\omega C_{DS}} = \frac{\Psi}{1+k} \frac{1}{1+i\omega\varepsilon\pi x/2\lambda_D\sigma},$$

where  $I$  is the current through the tube under consideration and is equal to  $\Psi$  divided by the total impedance of the tube. The potential across the double layer  $\Psi_{DL}(x)$  is a function of position on the electrode. This variation will give rise to a horizontal electric field  $E_H$  above the double layer. Over the large electrode this horizontal field is given by

$$\begin{aligned} E_{HL} &= \frac{1}{\sqrt{k}} \frac{d\Psi_{DL}}{dx} \\ &= -\frac{\Psi}{\sqrt{k}(1+k)} \frac{i\omega\varepsilon\pi/2\lambda_D\sigma}{(1+i\psi\varepsilon\pi x/2\lambda_D\sigma)^2}. \end{aligned}$$

The ions in the double layer will move in this horizontal field. Within the double layer the concentration of ions is sufficiently high that the fluid surrounding the ions moves with them. The velocity of the ions and the fluid  $v_{DL}$  is determined by the condition that the viscous drag across the layer per unit area ( $F/A$ ) is equal to the electrostatic force,

$$F/A = \rho_{DL} E_{HL} = \eta v_{DL} / \lambda_D.$$

Therefore

$$v_{DL} = \frac{\lambda_D \rho_{DL} E_{HL}}{\eta},$$

where  $\rho_{DL}$  is the charge per unit area of ions in the double layer over the large electrode and  $\eta$  is the viscosity of the water.

$\rho_{DL}$  is given by

$$\begin{aligned} \rho_{DL} &= \Psi_{DL} C_{DL} / (\delta x \sqrt{k}) \\ &= \Psi_{DL} \varepsilon / \lambda_D. \end{aligned}$$

Thus, the velocity of the fluid above the large electrode, averaging over an entire cycle, is given by

$$\langle v_{DL}(x) \rangle = \frac{1}{2} \operatorname{Re} \left\{ \frac{\lambda_D \rho_{DL} E_{HL}^*}{\eta} \right\} = -\frac{\nu_{L0}}{x} \Psi_0^2 \frac{(\omega x / \omega_0)^2}{[1 + (\omega x / \omega_0)^2]^2},$$

where

$$\nu_{L0} = \frac{\varepsilon}{2 \eta \sqrt{k} (1+k)^2},$$

$$\frac{\omega_0}{x} = \frac{2 \lambda_D \sigma}{\varepsilon \pi x}.$$

Similarly, above the small electrode

$$\langle v_{DS}(x) \rangle = -\frac{\nu_{S0}}{x} \Psi_0^2 \frac{(\omega x / \psi_0)^2}{[1 + (\omega x / \omega_0)^2]^2},$$

where

$$\begin{aligned} \nu_{S0} &= -\frac{\varepsilon \sqrt{k}}{2 \eta (1+1/k)^2} \\ &= -k^3 \nu_{L0}. \end{aligned}$$

For electrodes of the same size, i.e., when  $k=1$ , we obtain

$$\langle v_D(x) \rangle = -\frac{\varepsilon}{8 \eta x} \Psi_0^2 \frac{(\omega x / \omega_0)^2}{[1 + (\omega x / \omega_0)^2]^2},$$

which is in agreement with the equation used by Ramos [5].

The average velocity over the electrode surface can be obtained by integrating across the electrode. This average velocity is given by

$$V_{\text{ave}} = \frac{\int_{x_{\min}}^{x_{\max}} \langle v_D(x) \rangle dx}{x_{\max} - x_{\min}} = \frac{\Psi_0^2 \nu_0}{2(x_{\max} - x_{\min})} \left( \frac{(\omega \sqrt{x_{\min} x_{\max}} / \omega_0)^2 \left( \frac{x_{\max}}{x_{\min}} - \frac{x_{\min}}{x_{\max}} \right)}{\left( (\omega \sqrt{x_{\min} x_{\max}} / \omega_0)^2 + \frac{x_{\min}}{x_{\max}} \right) \left( (\omega \sqrt{x_{\min} x_{\max}} / \omega_0)^2 + \frac{x_{\max}}{x_{\min}} \right)} \right). \quad (1)$$

Thus the average velocity over the surface of the electrodes will be a maximum at a frequency of  $\omega_0 / \sqrt{(x_{\min} x_{\max})}$ .

If some values are inserted into the above equations the assumptions and approximations upon which these calculations are based can be reassessed. Taking  $\lambda_D = 30 \times 10^{-9}$  m,  $\sigma = 0.00123 \Omega^{-1} \text{m}^{-1}$  for a  $10^{-4}$  mol dm $^{-3}$  solution of NaNO $_3$  and  $k = 6.12$  (the value for the electrodes used in the experimental part of this work) we obtain  $\nu_{L0} = 2.82 \times 10^{-9}$  m $^2$  V $^{-2}$  s $^{-1}$  and  $\omega_0 = 0.03318$  rad s $^{-1}$  m.

For electrodes where  $x_{\min} = 1.6 \mu\text{m}$  and  $x_{\max} = 12.0 \mu\text{m}$  the maximum velocity at the electrode surface would be at a frequency of  $\omega_0 / \sqrt{(x_{\min} x_{\max})} = 7572$  rad s $^{-1}$  (i.e., 1.21 kHz). Therefore the average velocity at this frequency on the surface of the large electrode if a potential difference of 0.8 V $_{\text{rms}}$  is applied between the electrodes would be  $\langle v_{DL}(x) \rangle = 66.4 \mu\text{m s}^{-1}$ . The flow rate over the equivalent point on the small electrode would be a factor of  $k^3$  larger than that over the large electrode, thus  $\langle v_{DL}(y) \rangle = 15000 \mu\text{m s}^{-1}$ .

The flow induced in the bulk of the fluid cannot be simply determined from the forced flow at the surface of the electrodes. This bulk flow will not be the integration of the velocity of the fluid over the electrode surfaces, rather it will be determined by the flow pattern that forms. This flow pattern will form so as to minimize the dissipation of energy within the fluid. If we consider the onset of flow at the electrodes, over each electrode the shear will decay over a characteristic distance  $y_0$  into the bulk, where  $y_0$  is defined by

$$y_0 = \sqrt{\frac{\eta \tau}{d}},$$

where  $\tau$  is a time over which the shear is applied to the fluid, and  $d$  is the density of the fluid. If the time taken for water to flow over the electrode is taken as the unit of time, then over the large electrode the vorticity will diffuse  $k^2$  times further than over the small electrode. This means that the total momentum contained in the fluid over the large and small electrodes is the same, but the flow over the large electrode penetrates much further into the bulk of the fluid. However, two assumptions are made in the model which, if taken into account, would decrease the fluid velocity over the small electrode.

The model assumed that the ions in the double layer move a negligible distance across the surface of the electrode during one cycle, i.e., the double layer at one point on the electrode surface will not charge significantly due to charge flowing into it from another portion of the surface. On the large electrode this is a reasonable approximation; as with the above values the ions will only move a distance of 3.3 nm during half a cycle. However, the small electrode is only 3.9  $\mu\text{m}$  across and the ions will move 1.1  $\mu\text{m}$  in half a cycle. This will significantly discharge the horizontal charge distribution, thus reducing the rate at which the fluid flows over the small electrode.

It was assumed that the thickness of the double layer was the same on both electrodes. However, the charge density in the double layer over the small electrode will always be  $k$  times larger than that over the large electrode. At large potentials the double layer will be compressed, increasing the capacitance, and thus reducing the potential gradient across the surface of the electrode. Thus the double layer over the small electrode will be more compressed than that over the large electrode. Hence the fluid velocity over the small electrode will be decreased by this effect more than the fluid

velocity over the large electrode. The average charge density may be increased above the bulk concentration and this may significantly alter the thickness of the double layer.

It would be expected that the resulting bulk velocity of the fluid would vary with applied voltage and frequency in the same manner as the flow at the electrode surfaces. As well as comparing this model with the bulk fluid velocity in the cell, it can be tested by comparing it with the electrical impedance of the cell.

$$A = \frac{\sqrt{[(2\lambda_D\sigma)^2 + (\omega\varepsilon\pi)^2 + x_{\min}x_{\max}]^2 + [2\lambda_D\sigma\omega\varepsilon\pi(x_{\max} - x_{\min})]^2}}{(2\lambda_D\sigma)^2 + (\omega\varepsilon\pi x_{\min})^2}.$$

$\theta$  is given by

$$\tan \theta = \frac{2\lambda_D\sigma\omega\varepsilon\pi(x_{\max} - x_{\min})}{(2\lambda_D\sigma)^2 + (\omega\varepsilon\pi)^2 x_{\min}x_{\max}}$$

and  $l$  is the total length of the electrodes in the cell which was 23.5 cm.

By comparing the phase and amplitude of the current with that of the applied voltage it was possible to experimentally determine the magnitude and the phase of the impedance of the sample. Figure 7 shows the magnitude of the impedance as it varies with applied voltage for a few selected frequencies. The impedance shows no variation with the magnitude of the applied voltage from 0.001  $V_{\text{rms}}$  up to 0.1  $V_{\text{rms}}$ , at any frequency between 1 Hz and 100 kHz. This indicates that at these voltages the thickness of the double layer is not dependent upon the applied voltage.

Figure 8(a) shows the magnitude of the impedance of the cell as it varies with the applied frequency at a voltage below 0.1  $V_{\text{rms}}$ . The model is fitted to these data points by varying the conductance ( $\sigma$ ) and the effective thickness of the double layer ( $\lambda_D$ ). The values obtained from the fit are  $\sigma$

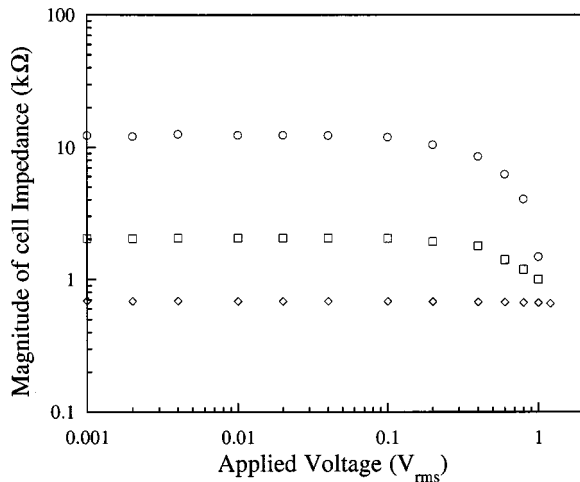


FIG. 7. Magnitude of the cell impedance for  $10^{-4} \text{ mol dm}^{-3}$   $\text{NaNO}_3$  as it varies with the applied potential at frequencies of 100 Hz ( $\circ$ ), 1 kHz ( $\square$ ), 10 kHz ( $\diamond$ ).

## V. COMPARISON OF THEORY WITH MEASURED IMPEDANCE

The impedance of the simple circuit shown in Fig. 6(b) can be calculated, by integrating across the surface of the electrodes, to give

$$Z = \frac{\pi(\sqrt{k} + 1/\sqrt{k})}{2l\sigma} \frac{\ln A - i\theta}{(\ln A)^2 + \theta^2},$$

where

$= 0.018 \Omega^{-1} \text{ m}^{-1}$  and  $\lambda_D = 4.56 \text{ nm}$ . Figure 8(b) shows the phase of the impedance as it varies with frequency at a voltage below 0.1  $V_{\text{rms}}$ . The solid line is the phase predicted by the model for the values of  $\sigma$  and  $\lambda_D$  determined by fitting the magnitude of the impedance. The difference between the observed and predicted phases arises from the approximation in the model that the ions do not move significantly across the surface of the electrode within half a cycle. As discussed earlier this is not true at the surface of the small electrode. The small electrode has the lower capacitance and so dominates the capacitive term which controls the phase of the impedance. However, while the model does not predict an identical phase to that observed, it does show similar features.

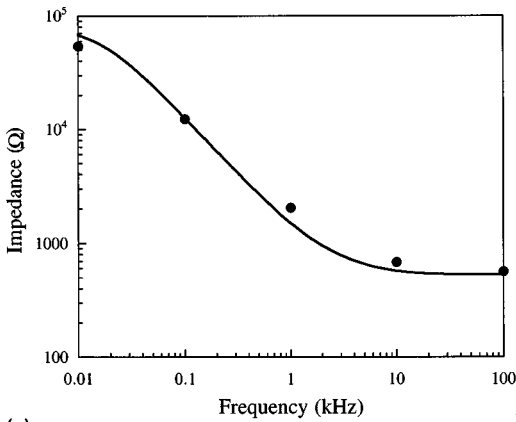
The value of  $\lambda_D$  determined from fitting the impedance is a factor of 7 less than that predicted by the Debye-Hückel approximation, while the conductivity is a factor of 14 greater than that expected for a  $10^{-4} \text{ M}$  solution of  $\text{NaNO}_3$ . These discrepancies show the importance of some further assumptions made in this simple model. The lower value of  $\lambda_D$  could be due to the diffuse layer compressing due to the potential placed across it and might also be due to charge in a Stern layer.

The larger conductivity could also be expected as the field lines are assumed to be semicircular which will not be the case particularly near the edge of the small electrode. The actual field lines will provide wider conduction paths with a lower resistance than their semicircular counterparts. The model also ignores conduction between different pairs of electrodes, which would decrease the measured resistance.

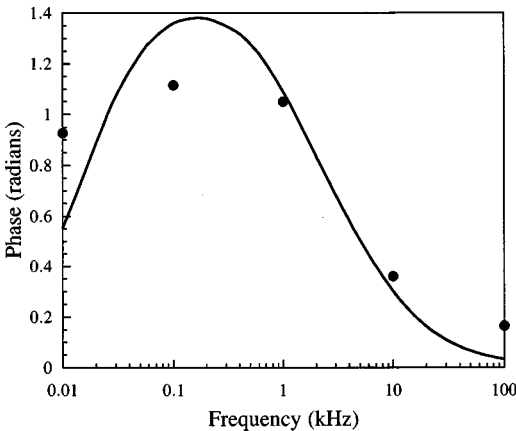
Perhaps the most important factor which might account for the discrepancies is that the conductivity and the double layer are both dependent on the salt concentration which is assumed to remain constant. However, in reality the salt concentration just above the electrodes may be significantly greater than the bulk value of  $10^{-4} \text{ mol dm}^{-3}$ .

The charge per unit area required in the double layer to produce a potential drop of  $\Psi_D$  is given by

$$\sigma_D = \frac{\Psi_D \varepsilon}{\lambda_D}$$



(a)



(b)

FIG. 8. (a) The predicted magnitude of the impedance (solid line) was fitted to the experimentally observed magnitude (open circles) by varying values for the conductance of the solution and the thickness of the double layer. (b) The phase predicted (solid line) and observed (open circles) using the values obtained from fitting the magnitude of the impedance.

This charge density can be directly related to an ion density at the surface. Thus the concentration of ions within the double layer must be given by

$$c = \frac{\Psi_D \varepsilon}{\lambda_D^2 e N_A}.$$

For a potential difference of 0.1 V this gives an ion concentration within the double layer of  $0.035 \text{ mol dm}^{-3}$ , i.e., much higher than the  $10^{-4} \text{ mol dm}^{-3}$  in the bulk fluid. This high surface concentration will diffuse away from the surface when a lower potential is placed across the double layer. Using a typical diffusion rate for  $\text{Na}^+$  and  $\text{NO}_3^-$  ions, at a frequency of 10 kHz, the distribution of ions would broaden to  $\sim 600 \text{ nm}$  in half a cycle. Thus when driving the electrodes at 10 kHz there would be a higher concentration of salt near the electrode surface which would decay away from the electrode over a length scale of half a micron. At lower frequencies it would decay over a larger distance.

Figure 7 shows that above 0.1 V the magnitude of the impedance decreases with applied voltage. Assuming that to first order the conductivity of the solution is independent of

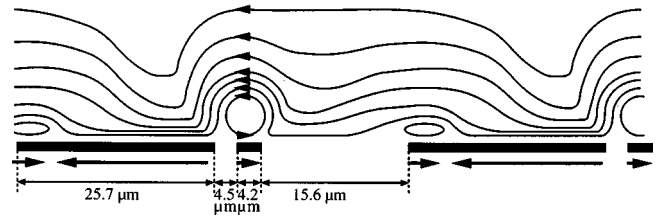


FIG. 9. A sketch of a possible flow profile over a series of pairs of electrodes. The flow over the small electrode forms a vortex as due to its small size; the shear does not penetrate as far into the medium as it does over the large electrode.

applied voltage, then this reduction in impedance must correspond to a compression of the double layer. The fact that the effect is larger at lower frequencies supports this conclusion, as at lower frequencies a higher fraction of the applied voltage is placed across the double layer. In this region the model would not be expected to make any quantitative predictions, as the thickness of the double layer would be different on each electrode, would differ across each electrode, and would vary as the potential varies within each cycle.

## VI. DISCUSSION

The fluid is observed to flow from the small electrode, across the narrow gap, towards the wide electrode [i.e., right to left as the electrodes are represented in Fig. 6(a)]. This means that the effect of the flow induced on the large electrode dominates over that induced on the small electrode. A possible flow profile is shown in Fig. 9, where the flow induced over the small electrode forms a vortex. Arrows under the electrodes show the flow induced at the electrode surfaces. The theory described earlier predicts that the flow will always be away from the gap between the electrodes, and will decrease in velocity with distance from that gap. Figure 9 includes some reverse flow on the electrodes which would be expected in an array of electrodes due to the interaction between the different pairs of electrodes. The fast flow predicted over the small electrode is shown to form a vortex over the small electrode. This small vortex is then surrounded by the overall flow produced by the larger electrode. This structure is supported by the fact that the flow over the small electrode would not diffuse very far into the bulk, whereas the flow over the large electrode has time to diffuse much further. It is not possible to extract the magnitude of the bulk flow from the theory without a quantitative analysis of the flow profile induced by the electrodes. However, since the bulk flow would be expected to vary with frequency and voltage in the same way as the average flow over the surface of each electrode, some comparisons can be made.

The model predicts that the maximum velocity should vary with  $\Psi^2$  [Eq. (1)]. Figure 5(a) shows that the experimentally observed velocities fit well to this aspect of the model. According to Eq. (1) the velocity should increase to a maximum value at a frequency determined by  $\omega_0 / \sqrt{(x_{\min} x_{\max})}$  (1.21 kHz for these electrodes), and then decrease again at higher frequencies. This is qualitatively observed; however, the position of the peak is not exactly as

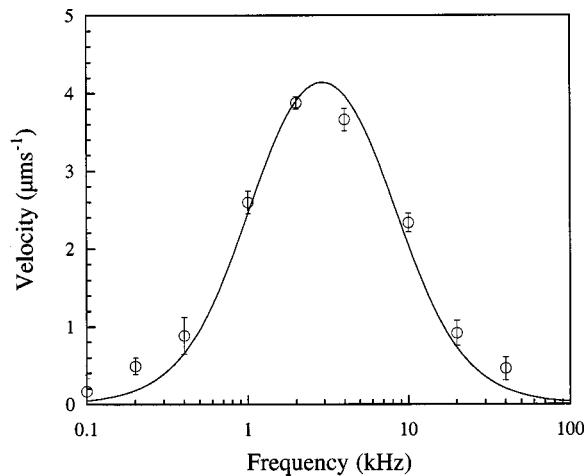


FIG. 10. The fluid velocity at an applied voltage of  $0.2 V_{\text{rms}}$  as it varies with frequency, fitted with Eq. (1). The width of the peak agrees well with the theory, suggesting that the theory correctly describes the variation of velocity with frequency at low applied potentials.

predicted. This is due to the fact that  $\omega_0$  is inversely proportional to the capacitance. As has already been discussed, the capacitance is poorly defined within the model.

According to the theory, the width of the peak should only be proportional to its position and dependent on the value of  $x_{\text{max}}/x_{\text{min}}$ . At an applied voltage of  $0.2 V_{\text{rms}}$ , where the double layer is not compressed significantly by the applied potential, the shape of the peak predicted by the model fits the observed curve reasonably well as shown in Fig. 10. However, as the applied voltage is increased, the position of the peak moves to lower frequencies, and the width of the peak increases as shown in Figs. 5(b) and 4. This is due to the fact that the potential across the double layer is greater at lower frequencies, and so the double layer is more compressed at lower frequencies as observed with the impedance measurements (Fig. 7). This compression increases the capacitance, meaning more time is required to achieve the same potential drop across the double layer as would be observed with an uncompressed layer, thus a particular velocity is observed at lower frequencies than if the double layer did not compress. This effect raises the velocity at lower frequencies, thus broadening the peak and shifting it to lower frequencies. In fact some slight broadening can even be observed at  $0.2 V_{\text{rms}}$  (Fig. 10).

## VII. CONCLUSION

Water has been pumped across an array of electrodes by the application of an ac electric field. Above a static electrode array at distances greater than the period of the electrodes ( $50 \mu\text{m}$  in the case considered here), uniform fluid flow is generated. A peak velocity was observed at a frequency of a few kHz. Velocities up to  $75 \mu\text{m s}^{-1}$  were observed at voltages of up to  $1.2 V_{\text{rms}}$ .

A simple model has been presented and compared to the observed fluid velocities. This model was in qualitative agreement with the experimental observations. A number of approximations have been highlighted which significantly effect the predictions of the model. In order to improve the model these approximations would need to be addressed. It would be necessary to include a description of the compression of the double layer, allowing its capacitance to vary with the instantaneous potential across it, possibly accounting for a Stern layer. The spatial and possibly even temporal variation in salt concentration would need to be modeled. An accurate description of the field lines and hence the current flow within the bulk solution would have to be made. Also the movement of the ions within the double layer over the small electrode would need to be accounted for. Finally a hydrodynamic model of the bulk fluid flow arising from the flow on the surface of the electrodes would have to be generated. Theoretical contributions in this area would be welcomed. It should also be noted that for a model intended to describe an experiment where higher potentials were used, the injection of charge at the electrodes would also have to be considered.

The electrode array is very simple, and requires only two electrical connections to drive it. The voltages required are low and easily generated. The model predicts that the flow rate would be inversely proportional to the size of the electrodes. A plug flow profile is observed, where the shear is all contained near the surface and any pressure opposing the flow determines the flow profile of the bulk. This flow profile is ideally suited to pumping fluids through small channels where the shear forces at the walls of the channel usually provide the dominant resistance to the flow. The only length scale inherent in the technique is the thickness of a double layer. Hence this pumping technique appears applicable to fluid control on submicrometer length scales.

## ACKNOWLEDGMENTS

A.B.D.B. thanks the Oppenheimer Trust and the Newton Trust for research funding.

- [1] G. Fuhr, T. Schnelle, and B. Wagner, *J. Micromech. Microeng.* **4**, 217 (1994).
- [2] A. V. Lemoff and A. P. Lee, *Sens. Actuators B* **63**, 178 (2000).
- [3] J. S. Jang and S. S. Lee, *Sens. Actuators A* **80**, 84 (2000).
- [4] S. Shoji and M. Esashi, *J. Micromech. Microeng.* **4**, 157 (1994).
- [5] A. Ramos, H. Morgan, N. G. Green, and A. Castellanos, *J. Colloid Interface Sci.* **217**, 420 (1999).
- [6] N. G. Green, A. Ramos, and H. Morgan, *J. Phys. D* **33**, 632

(2000).

- [7] N. G. Green, A. Ramos, A. González, H. Morgan, and A. Castellanos, *Phys. Rev. E* **61**, 4011 (2000).
- [8] A. González, A. Ramos, N. G. Green, A. Castellanos, and H. Morgan, *Phys. Rev. E* **61**, 4019 (2000).
- [9] A. Ajdari, *Phys. Rev. E* **61**, R45 (2000).
- [10] R. J. Hunter, *Foundations of Colloid Science* (Oxford University Press, Oxford, 1992).